Structure, Vol. 11, 1265–1277, October, 2003, ©2003 Elsevier Science Ltd. All rights reserved. DOI 10.1016/j.str.2003.09.003

Structural Basis for the Dual Thymidine and Thymidylate Kinase Activity of Herpes Thymidine Kinases

Anna Gardberg,[1] Ludmilla Shuvalova,[1] Christian Monnerjahn,[2] Manfred Konrad,[2] and Arnon Lavie[1,*]
[1]University of Illinois at Chicago
Department of Biochemistry and Molecular Biology
1819 West Polk St.
Chicago, Illinois 60612
[2]Max Planck Institute for Biophysical Chemistry
Department of Molecular Genetics
37070 Göttingen
Germany

Summary

Crystal structures of equine herpesvirus type-4 thymidine kinase (EHV4-TK) in complex with (i) thymidine and ADP, (ii) thymidine and SO_4 and the bisubstrate analogs, (iii) TP_4A, and (iv) TP_5A have been solved. Additionally, the structure of herpes simplex virus type-1 thymidine kinase (HSV1-TK) in complex with TP_5A has been determined. These are the first structures of nucleoside kinases revealing conformational transitions upon binding of bisubstrate analogs. The structural basis for the dual thymidine and thymidylate kinase activity of these TKs is elucidated. While the active sites of HSV1-TK and EHV4-TK resemble one another, notable differences are observed in the Lid regions and in the way the enzymes bind the base of the phosphoryl-acceptor. The latter difference could partly explain the higher activity of EHV4-TK toward the prodrug ganciclovir.

Introduction

Herpes simplex virus type-1 thymidine kinase (HSV1-TK) and equine herpesvirus type-4 thymidine kinase (EHV4-TK) catalyze the reversible phosphorylation of thymidine (Thy) to thymidine monophosphate (TMP) as well as that of TMP to thymidine diphosphate (TDP), using ATP as a phosphoryl donor according to the following reaction scheme (Chen and Prusoff, 1978; Chen et al., 1979):

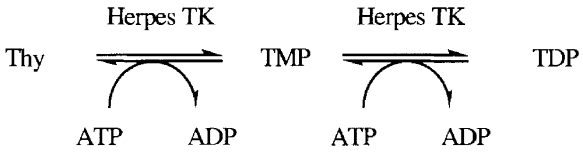

Scheme 1.

In addition to this physiological dual thymidine kinase and thymidylate kinase activity, the herpes thymidine kinases can phosphorylate pyrimidine nucleosides, pyrimidine nucleoside monophosphates, and several nucleoside analogs (Chen and Prusoff, 1978; Chen et al., 1979; Elion et al., 1977). This wide substrate specificity gives these kinases their medicinal relevance.

The best studied anticancer gene therapy strategy is the HSV1-TK/ganciclovir system. Suicide gene therapy of cancers and graft-versus-host disease (GVHD) prevents replication of targeted cells via the activation of a prodrug by an exogenously introduced enzyme. In this system, the HSV1-TK enzyme renders mammalian cells sensitive to ganciclovir (GCV). GCV is phosphorylated by HSV1-TK to GCV-monophosphate (GCV-MP) and subsequently to GCV-diphosphate (GCV-DP) (Matthews and Boehme, 1988) and cytotoxic GCV-triphosphate (GCV-TP) by cellular enzymes (Reardon, 1989; St. Clair et al., 1987). Improving such therapies, then, depends on improving the prodrug, the enzyme, or the method of delivery of either the prodrug or the enzyme.

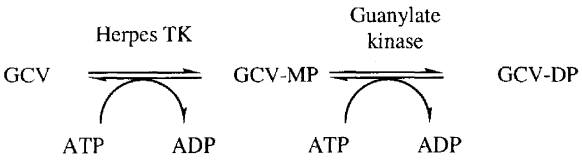

Scheme 2.

Human nucleoside kinases activate GCV much less efficiently than does HSV1-TK, so GCV's toxicity toward non-HSV1-TK-transduced cells is extremely low. EHV4-TK is 36% identical to HSV1-TK, and a study on human and murine cell lines demonstrated the superiority of EHV4-TK over HSV1-TK at activation of GCV (Loubiere et al., 1999).

We wish to understand EHV4-TK's superiority over HSV1-TK at phosphorylating GCV. We also strive to understand the dual thymidine and thymidylate kinase activity of EHV4-TK (Thy to TMP, TMP to TDP) and how it compares to that of HSV1-TK; such dual activity is absent in other known nucleoside kinases. The Michaelis complex of the thymidine kinase reaction has three phosphate groups—either all from ATP or two from ADP and one from TMP, depending on the reaction direction. In contrast, the thymidylate kinase complex has four phosphate groups bound to the active site—three from ATP and one from TMP, or two each from ADP and TDP. An hypothesis for HSV1-TK's dual activity has been offered (Wild et al., 1997), but known HSV1-TK structures do not give information on the four-phosphate conformation of the enzyme (Bennett et al., 1999; Champness et al., 1998; Prota et al., 2000; Vogt et al., 2000; Wild et al., 1997). We would also like to understand the structural features of the viral TKs that enable dual activity toward Thy but not toward medicinal compounds.

The questions we pose are as follows: how does the same enzyme accommodate substrates of different size and charge (i.e., Thy or TMP)? For example, do the catalytic residues change conformation when interacting with Thy versus TMP? Or does the donor nucleotide and/or the acceptor nucleoside/nucleotide occupy a different position in the active site? To address these questions,

*Correspondence: lavie@uic.edu

Table 1. Data Collection and Refinement Statistics

	EHV4-TK + SO_4-Thy	EHV4-TK + ADP-Thy	EHV4-TK + TP_4A	EHV4-TK + TP_5A	HSV1-TK + TP_5A
PDB deposition code	1P6X	1P72	1P73	1P75	1P7C
Data Collection Statistics					
Space group	$C222_1$	$C222_1$	$P2_12_12$	$P2_12_12$	$C222_1$
Unit cell (Å)					
a	111.65	112.30	111.35	106.80	113.22
b	121.55	121.01	118.29	117.20	117.85
c	118.83	118.81	122.65	124.94	108.40
Resolution	2.0	2.0	2.7	3.0	2.1
Observed reflections	423469	242846	902706	613603	198478
Unique reflections	54599	47461	45176	31559	41672
Completeness (%)					
Overall/last shell	99.6/99.8	96.8/96.9	98.4/91.0	96.8/88.9	97.9/97.9
I/sigma(I)					
Overall/last shell	13.12/2.72	18.2/2.7	14.6/2.9	12.8/5.1	13.2/3.9
R_{sym} (%)					
Overall/last shell	9.6/46.4	6.2/32.1	9.7/37.8	11.8/26.5	7.2/31.9
Molecules/asymmetric unit	2	2	4	4	2
Refinement Statistics					
Resolution range (Å)	30–2.0	25–2.1	30–2.7	30–3.02	35.9–2.1
Reflections with $F > 0\sigma$					
Working	49207	41415	40082	27616	37137
Test	5392	4541	4439	2988	4142
R_{cryst} (%)	18.7	18.4	21.3	20.2	23.9
R_{free} (%)	23.7	23.2	27.6	29.8	28.5
Number of:					
Protein atoms	5213	5112	9788	10157	4655
Nucleotide atoms	44	88	204	312	77
Water atoms	452	449	147	155	299
Sructural sulfate	20	45	55	80	N/A
RMS deviations					
Bond lengths (Å)	0.012	0.012	0.010	0.013	0.011
Bond angles (°)	1.324	1.343	1.420	1.604	1.429
Average B (Å^2)	36.3	28.6	38.6	44.1	27.8
Main chain	34.7	27.2	38.4	43.8	27.1
Side chain	34.7	28.2	38.7	44.2	27.7
Water molecules	44.1	37.1	38.3	34.9	34.4
Nucleotides	31.4	29.7	45.1	47.0	28.0
Structural sulfate	43.0	51.7	59.0	63.5	N/A

R-Factor $= \Sigma||F_{obs}| - |F_{calc}||/\Sigma|F_{obs}|$

we crystallized EHV4-TK in complex with physiological substrates and analogs. To visualize the three- and four-phosphate conformations of the active site, the ideal complexes of the enzymes would be of AppNHp (a non-hydrolyzable ATP analog) with Thy or TMP, respectively. Numerous attempts to obtain such structures, however, were not successful. As an alternative, we obtained and studied structures of TP_4A and TP_5A complexes, which can be viewed as the bisubstrate analogs of TMP-ADP and TMP-ATP, respectively.

Results

Overall Structure of EHV4-TK

Data collection and refinement statistics are presented in Table 1. EHV4-TK consists of 352 amino acid residues with a calculated molecular weight of 38.8 kDa. Since we could not obtain reproducible crystals with the full-length EHV4-TK construct, we produced a variant (EHV4-TK-Δ22N) lacking the first 22 N-terminal residues that is kinetically similar to the full-length enzyme (see Experimental Procedures). This truncated version, henceforth referred to as EHV4-TK, consists of 330 amino acids and has a calculated molecular weight of 36.5 kDa. Two different orthorhombic crystal forms were obtained for EHV4-TK—$C222_1$ and $P2_12_12$—and packing interactions differed between the two forms. As expected from analogy to other members of the herpesvirus TKs and of the thymidylate kinase (TMPK) family of proteins, EHV4-TK is homodimeric, as evidenced from gel filtration experiments (data not shown) and from analysis of the monomer-monomer interactions in the crystal structure. Each monomer consists of a five-stranded parallel β sheet core surrounded by five core α helices and five peripheral helices (Figure 1A). The dimer interface is roughly triangular in shape; it is created by three helices from each monomer (α4, α7, and α11) stacking against each other.

Homology to other enzymes, especially to HSV1-TK (Figure 1B), suggests three regions to be of particular importance for the function of EHV4-TK (Wild et al., 1997). The first critical region is the phosphate binding

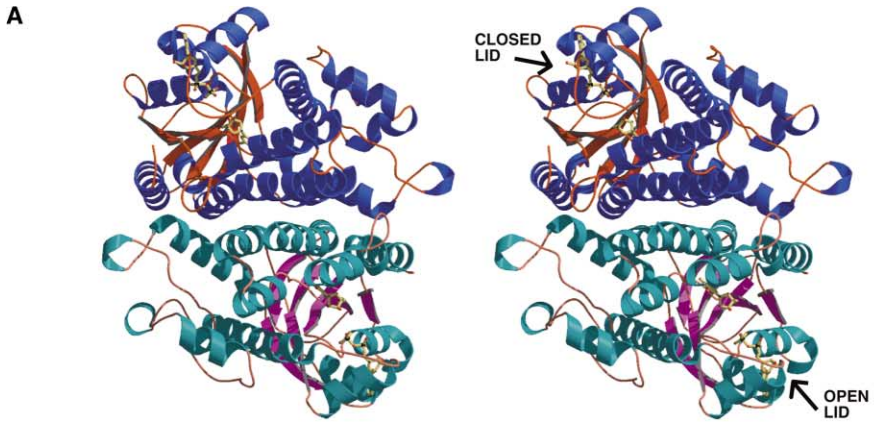

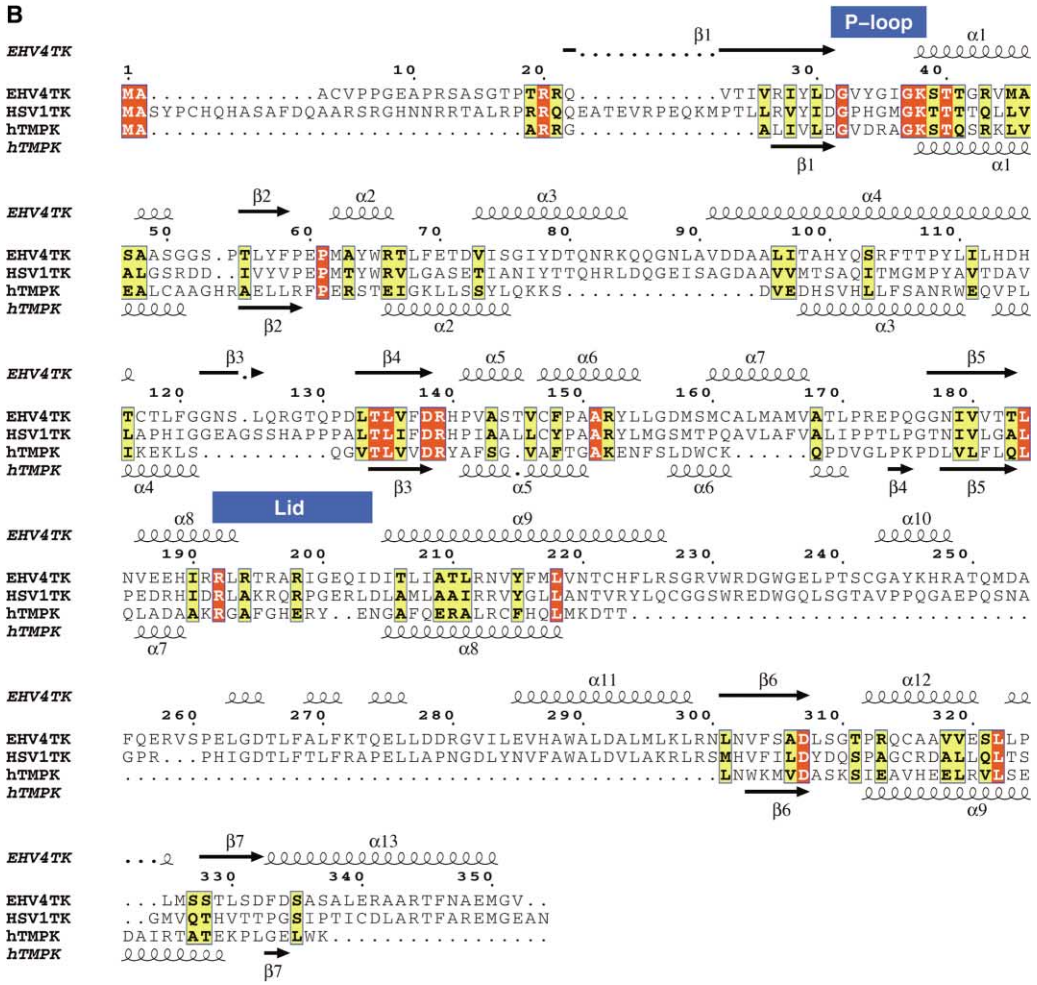

Figure 1. Structure of EHV4-TK

(A) A ribbon diagram of the ADP-Thy complex is shown in stereo, with ball-and-stick portrayals of the substrates. One of the monomers has the open Lid conformation, the other the closed conformation. Only in the latter is the essential Arg196 at an interacting distance to the ADP molecule, making the closed Lid conformation the catalytically relevant conformation.

(B) The sequences of EHV4-TK and HSV1-TK exhibit 35% identity; while hTMPK has only 9% sequence identity with EHV4-TK (Brown et al., 1998), its crystal structure overlaps well with many similar secondary structural elements. The Lid and P loop, essential for catalysis, are highlighted. All structure figures were made with Bobscript (Esnouf, 1997; Kraulis, 1991) and Raster3D (Merrit and Murphy, 1994). The sequence alignment of EHV4-TK and HSV1-TK was performed with CLUSTAL W (Thompson et al., 1994), that of EHV4-TK and hTMPK was based on a structural alignment in O (Jones et al., 1991).

loop (P loop), comprising the GX_4GKS/T motif (residues 32–39 in full-length EHV4-TK). The main chain nitrogen atoms of Gly35, Gly37, Lys38, and Ser39 hydrogen bond to the β-phosphate of ADP (or to the corresponding atoms in the TP_4A and TP_5A structures). The side chain oxygen atom of Thr40 hydrogen bonds to the α-phosphate. The second conserved region, which contains the DRY/H/F motif, is present in EHV4-TK as $D_{138}R_{139}H_{140}$. Residue Asp138 is expected to bind to the ATP/ADP via a magnesium ion, which is absent in our structures. Arg139 appears to be vital to catalysis, as its guanidinium moiety binds to an oxygen atom of the transferred phosphate group. The third conserved region, known as the Lid, is a flexible loop comprising residues 192–205 that can close over an occupied active site. In this way, one of the Lid arginine residues (Arg196) comes into close proximity to the phosphate groups.

Complexes Examined

The ADP-Thy and SO_4-Thy Structures

The ADP-Thy structure represents a "dead end" complex in which the active site holds one product (ADP) and one reactant (Thy). Despite its mixed character, this complex allows the observation of the nucleophilic 5′-Thy-hydroxyl and the two phosphates of ADP. Comparing the SO_4-Thy complex to the isomorphous ADP-Thy complex reveals that the sulfate ion occupies the β-phosphate site. The asymmetric unit of each crystal structure comprises a dimer whose monomers are denoted A and B. For insight into the dual activity of EHV4-TK, we must compare these structures to those that model the three- and four-phosphate configurations.

The EHV4-TK TP_4A and TP_5A Structures

These structures adopt the same space group and most of their general features are identical. Each asymmetric unit comprises two dimers whose monomers are denoted A, B, C, and D. Figure 2 illustrates the binding regions of these complexes. The TP_4A complex is expected to mimic a three-phosphate conformation, either the "reactant" state (ATP-Thy) or the "product" state (ADP-TMP), plus a linker (Scheme 3).

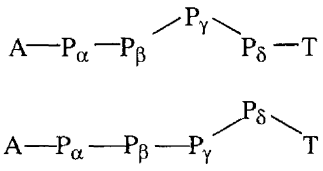

Scheme 3. Two Possible Configurations for the TP_4A Molecule: ADP-Linker-TMP and ATP-Linker-Thy

An examination of the binding pocket of this complex led us to conclude that our EHV4-TK-TP_4A structure is a mimic of an ADP-TMP state. This conclusion is derived from the observation that the γ-phosphate makes no hydrogen bonds to the surrounding protein (Figure 2A). Furthermore, the γ-phosphate would, in a closed Lid (i.e., catalytically active state) conformation, displace Arg196 (see Lid discussion below). These facts suggest that the γ-phosphate functions as a linker between an ADP moiety and a TMP moiety and that the TP_4A complex is a mimic of the product state. A simulated annealing omit map of TP_4A is shown in Figure 3A.

The TP_5A molecule was designed to mimic a four-phosphate conformation, that is, either the "reactant" state (ATP-TMP) or the "product" state (ADP-TDP), plus a linker (Scheme 4). We observe at least two different conformations of the TP_5A molecule (not equivalent to the two possible TP_5A configurations shown in Scheme 4) in monomers A and C, and assigned them equal occupancy in our modeling. The electron density in monomers B and D is more difficult to interpret, and we will not address them here.

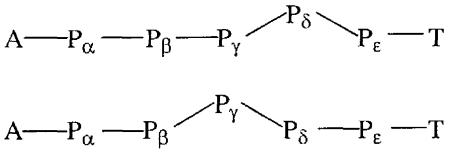

Scheme 4. Two Possible Conformations for the TP_5A Molecule: ATP-Linker-TMP, ADP-Linker-TDP

The main conformation of TP_5A in monomer C is shown in Figure 2B and the two conformations in simulated annealing omit density are shown in Figure 3B. In all of the monomers in the TP_5A complex the Lids are in an open conformation. Modeling a closed Lid conformation reveals a steric clash between the δ-phosphate (relative to the adenine base) and the closed Lid (Figure 2B). Since the δ-phosphate is the only phosphate group in TP_5A that makes no protein interactions, we conclude that it functions as the linker phosphate. Therefore, in contrast to the TP_4A complex, the TP_5A complex mimics the "reactant" state: ATP-linker-TMP. In summary, TP_5A mimics ATP + TMP, but not ADP + TDP, and TP_4A mimics ADP + TMP, but not ATP+Thy.

HSV1-TK in Complex with TP_5A

Here the asymmetric unit is a dimer and we have denoted its monomers as A and B. Surprisingly, the two monomers in this complex bind to different substrates—one to TP_5A and the other to thymidine and a sulfate ion. We attribute the presence of thymidine to residual quantities of the nucleoside remaining following purification. Analysis of crystal contacts reveals that the presence of a TP_5A molecule in monomer B is not compatible with the crystal packing. Thus, only a dimer of mixed nature (i.e., TP_5A in one monomer, Thy in the other) can incorporate into the growing crystal. A schematic diagram of the interactions made by TP_5A in this complex is presented in Figure 2C and a simulated annealing omit map of the inhibitor in Figure 3C. Again the δ-phosphate seems to be the linker—it makes no hydrogen bonds to the binding pocket and only one to the closed Lid. As in the EHV4-TK-Thy-SO_4 structure, the sulfate group bound to the second monomer of HSV1-TK sits in the position normally occupied by the β-phosphate group. An overlay of monomers of EHV4-TK and HSV1-TK is shown in Figure 4A.

The Conformations of the Lid Region

The Lid region, a conserved motif among nucleoside and nucleoside monophosphate kinases, is usually highly flexible and alters its conformation from an open state in the absence of substrate in the ATP site, to a closed state upon ATP binding (Ostermann et al., 2000; Sekulic et

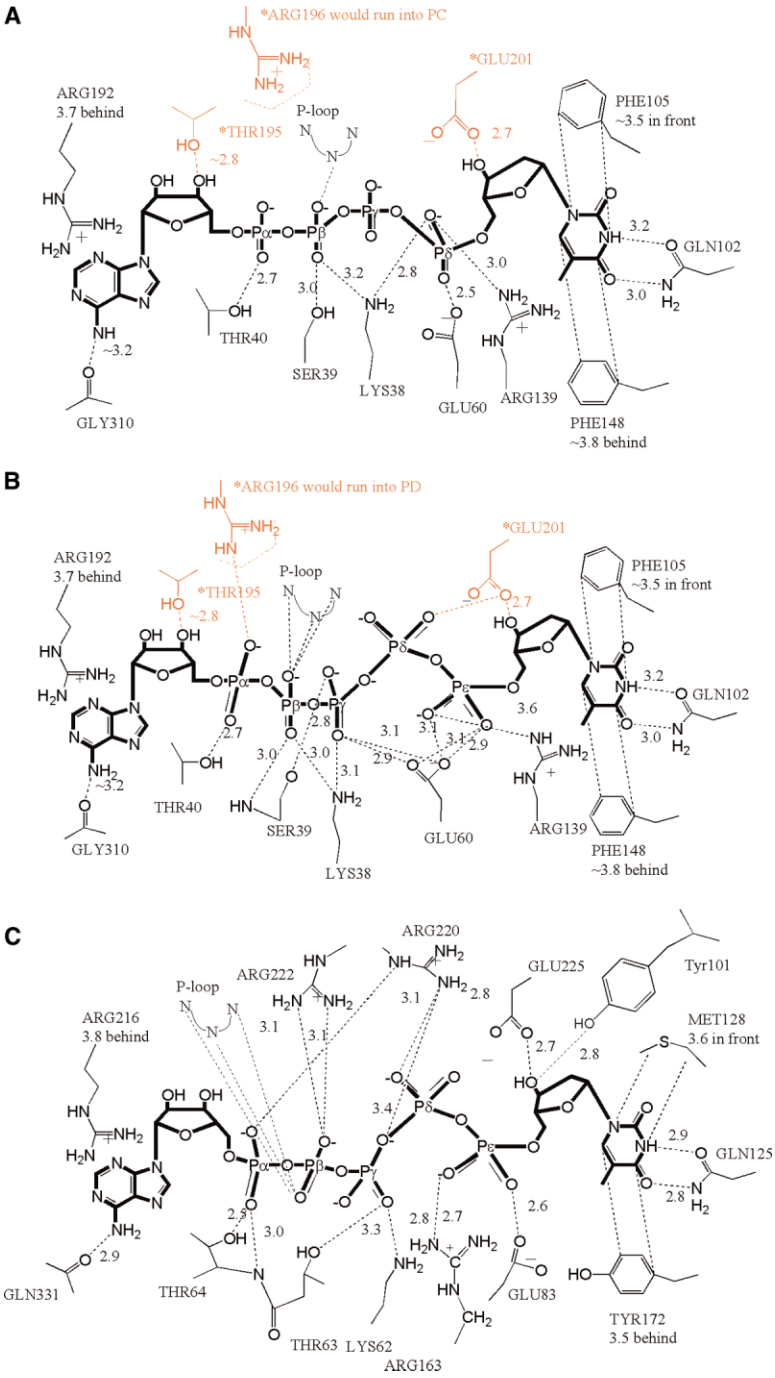

Figure 2. Schematic Diagram Showing the Interactions Made by TP_4A and TP_5A

Due to the all-open Lid conformations in the EHV4-TK TP_4A and TP_5A complex structures (but closed in the HSV1-TK structure), in (A) and (B) we modeled the closed-Lid conformation as observed in the EHV4-TK/ADP-Thy complex (simulated contacts shown in red and marked with an asterisk).

(A) EHV4-TK complexed with TP_4A. Owing to the 0.4 Å displacement of the β-phosphate, there is only one hydrogen bond to the P loop.

(B) EHV4-TK complexed with TP_5A, where only the mechanistically relevant conformation is shown.

(C) HSV1-TK complexed with TP_5A.

al., 2002; Vonrhein et al., 1995). In most of these kinases, mammalian thymidylate kinases being a notable exception, this conformational change brings one or more arginine residues into the close proximity of the substrate phosphates, enabling the arginine to play a direct role in catalysis. Since in all of our EHV4-TK structures the ATP site is occupied we expected to observe only the closed Lid conformation. However, in the ADP-Thy and SO_4-Thy structures, only one of the two monomers in the asymmetric unit is in the closed conformation, the other being in the open conformation. Moreover, in the TP_4A and TP_5A structures, the Lid regions of all four monomers in the asymmetric unit are in the open conformation. The conformations are summarized in Table 2.

Examination of the crystal packing in the ADP-Thy and SO_4-Thy structures suggests that the open Lid conformation in these complexes could be a crystallization artifact, due to the interaction of two residues at the edges of the Lid, Arg194 and Ile203, with symmetry-related Gly128 and Arg127, respectively. Overlaying the closed-Lid conformation from ADP-Thy or SO_4-Thy

A

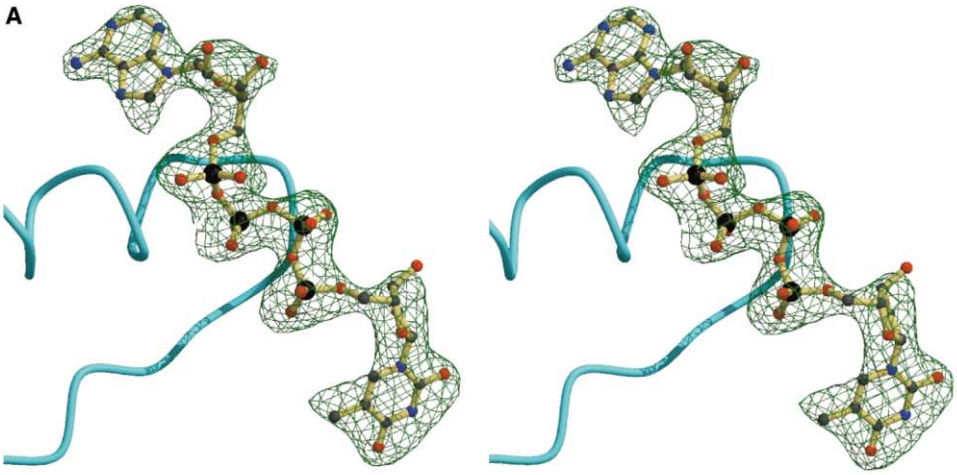

B

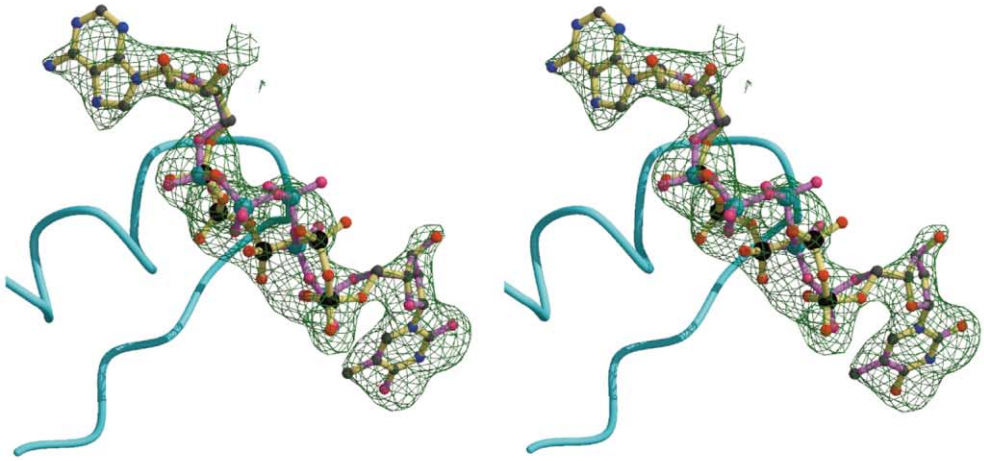

C

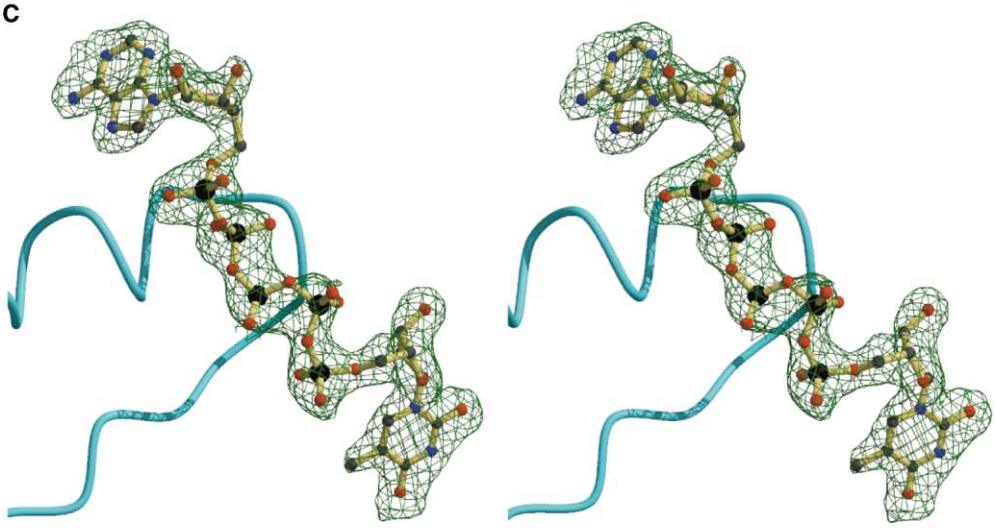

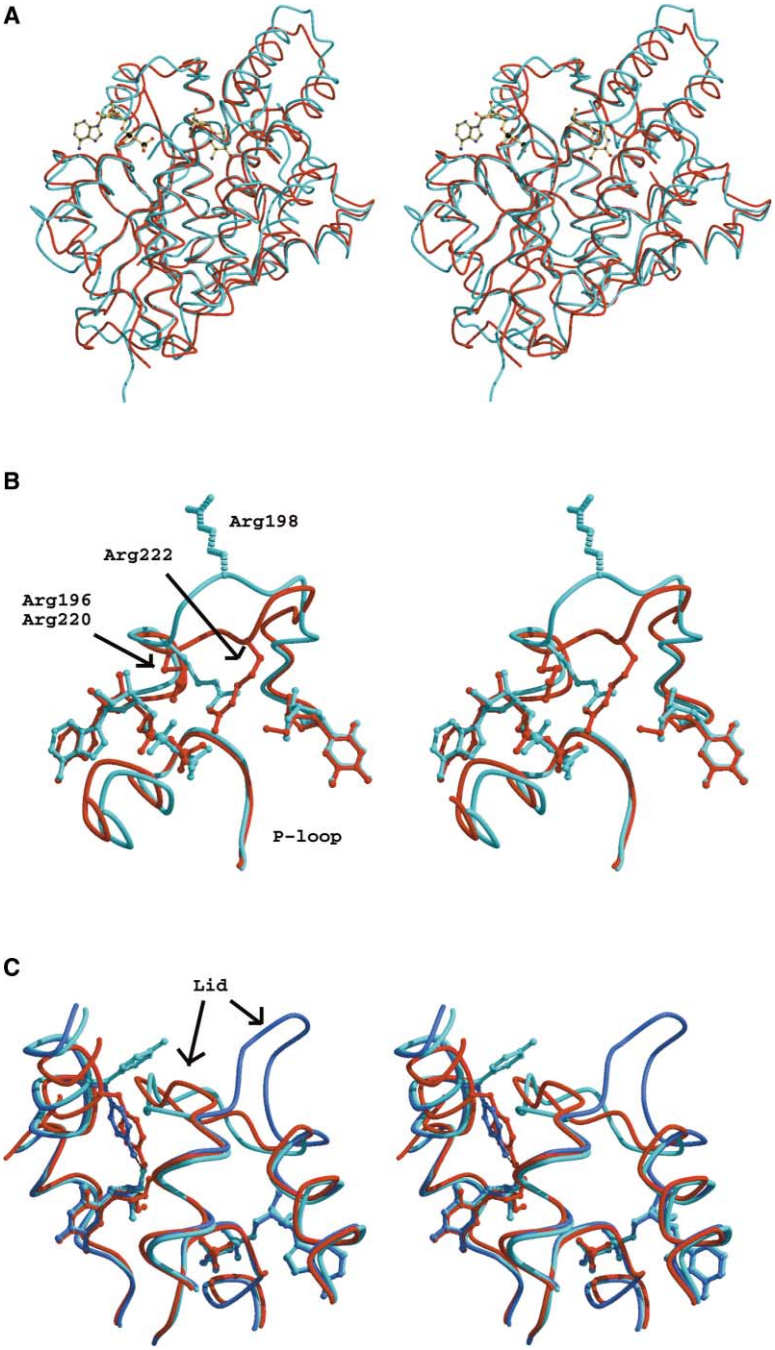

Figure 4. Comparison of EHV4-TK to HSV1-TK

(A) The structures of EHV4-TK (cyan) and HSV1-TK (Wild et al., 1997) (red) overlay well with a RMSD of 1.45 Å over 269 compared atoms.

(B) While the P loops and ligands of the EHV4-TK-ADP-Thy (cyan) HSV1-TK-ADP-Thy (red) overlap smoothly, the Lid regions follow different paths. This puts the putative conformation of EHV4-TK's Arg198 at a position that does not allow it to interact with the ADP molecule, in contrast to the homologous Arg222 of HSV1-TK. The dashed bonds for EHV4-TK-Arg198 signify that the residue is modeled as its most probable rotamer, but not refined owing to ambiguous electron density.

(C) The closed-Lid state HSV1-TK-Thy-ADP (red) and EHV4-TK-Thy-ADP (cyan) contrasted with one another and with open-Lid EHV4-TK-ADP-Thy (blue). The closed Lid state of EHV4-TK prevents Tyr78 from interacting with the thymidine molecule, while in HSV1-TK this interaction is maintained in the closed Lid state.

structures on the open-Lid TP_4A and TP_5A complex structures reveal that in this case it is not symmetry related molecules that prevent Lid closure, but rather that the linker phosphate in these analogs would sterically clash with the side chain of Arg196 of the Lid region. Least-squares alignment of the two monomers in the ADP-Thy or SO_4-Thy structures demonstrates that varying the conformation of the Lid region in these com-

Figure 3. Omit Density of Inhibitors

After refinement was completed, the bound inhibitor models were omitted for a refinement cycle to eliminate model bias. The 2.5 sigma difference density from this cycle ($F_o - F_c$) is shown superimposed on the final, refined inhibitor models.

(A) EHV4-TK-TP_4A, monomer A.

(B) EHV4-TK-TP_5A, monomer C. In this complex we observed electron density not accountable by a single conformation for the phosphate groups; the mechanistically relevant conformation is shown with yellow bonds.

(C) HSV1-TK-TP_5A, monomer A.

Table 2. The Lid Regions of All Four Monomers

Complex	Monomer A	Monomer B	Monomer C	Monomer D
EHV4-TK Thy-ADP	open	closed		
EHV4-TK Thy-SO4	open	closed		
EHV4-TK-TP_4A	open	open	open	open
EHV4-TK-TP_5A	open	open	open	open
HSV1-TK-TP_5A	closed	closed		

plexes does not change the positions of the substrates, so the predominantly open Lid conformations we observe do not affect our structural interpretation. Also, while the open Lid conformation might reflect a state in which the ATP site is not occupied, it is the closed Lid conformation that more correctly reflects the presence of ADP or sulfate in the ATP site. Though the main chain atoms and most of the Cβ carbons of the Lid region are clearly defined by electron density in the simulated-annealing omit maps, the electron density is not clear enough to position the entirety of all of the side chains in either the open or the closed Lids.

In contrast to the all-open Lid conformation in the EHV4-TK/TP_4A and TP_5A complex structures, the Lids of both monomers in the HSV1-TK/TP_5A structure adopt the closed conformation and are similar to the Lid regions previously reported in HSV1-TK structures (Bennett et al., 1999; Champness et al., 1998; Prota et al., 2000; Vogt et al., 2000; Wild et al., 1997). The superimposed structures of the Lid regions for the two enzymes are shown in Figure 4B. The different trace adopted by the Lid sequence of HSV1-TK makes its closed Lid conformation compatible with the presence of the linker phosphate, while a steric clash would result from a closed Lid conformation in the EHV4-TK/TP_5A complex. In HSV1-TK, Lid arginines Arg220 and Arg222 point toward the substrates. In the EHV4-TK/SO_4-Thy complex (and, to the extent to which we can visualize its electron density, in the EHV4-TK/ADP-Thy complex), one of these conserved arginine residues, Arg196, has strong electron density that shows it to be in a position enabling interaction with the β-phosphate of ATP/ADP when in the closed conformation (Figure 4B). While we cannot model the tip of the side chain of EHV4-TK's other conserved arginine, Arg198, with confidence, it seems to be pointing away from the active site. This calls into question its role in catalysis.

The Thy/TMP/TDP Binding Site

The Thy binding region of EHV4-TK is shown schematically in Figure 2. A conserved glutamine residue, Gln102, positions the phosphoryl-accepting substrate via two side-by-side hydrogen bonds. The thymine base makes stacking interactions with nearby aromatic rings, Phe105 and Phe148. In the more relevant closed-Lid conformation, the O3′ atom of the Thy deoxyribose binds to the conserved glutamic acid residue Glu201. The sugar O5′ atom in the ADP-Thy complex, the δ-phosphate in the TP_4A complex, and the ε-phosphate in the TP_5A complex interact with the conserved Glu60. As a consequence of the bulkier phosphate group in TP_4A and TP_5A, this residue sits lower in the binding pocket than it does in the ADP-Thy and SO_4-Thy structures. The close proximity of Glu60 and the phosphate groups in TP_4A and TP_5A suggest that the side chain is protonated. This is consistent with its role as a base in the Thy → TMP reaction accepting the O5′ proton, and as an acid in the reverse reaction. In all of the monomers of our TP_5A structure, the thymidine's deoxyribose and the ε-phosphate (but not the thymine base itself) are translated by 0.8–1.0 Å relative to those in the ADP-Thy, SO_4-Thy, and TP_4A structures.

A notable difference between HSV1-TK and EHV4-TK in the Thy/TMP/TDP binding site lies in the position of a conserved tyrosine residue. Homologous tyrosine residues in other deoxynucleoside kinases have been implicated with the kinases' ability to partially discriminate between ribo- and deoxyribo-substrates (Johansson et al., 2001). In EHV4-TK's open-Lid state, Tyr78 occupies a very similar position to the HSV1-TK's Tyr101. In EHV4-TK's closed-Lid state, however, Tyr78 is in a displaced conformation (Figure 4C). The closed-Lid state of EHV4-TK, which we interpret as the catalytically relevant state, is not compatible with the tyrosine side chain pointing toward the nucleoside, and the tyrosine must rotate away as the Lid closes. This would suggest that EHV4-TK would be less able than HSV1-TK to discriminate between ribo- and deoxyribonucleosides. Surprisingly, this difference between the tyrosine side chain conformation of HSV1-TK and EHV4-TK does not affect the relative rates of ribonucleoside phosphorylation by the two enzymes: Urd and Cyd are phosphorylated by both enzymes, though not as well as dUrd and dCyd (data not shown).

The ATP/ADP Binding Site

ADP binds to EHV4-TK mainly through hydrogen bonds, but also via π-overlap with Arg192. The β-phosphate occupies the cavity that is formed by the P loop. In the sulfate derivative structure presented here, the sulfate occupies this β-phosphate position. TP_4A, a bisubstrate analog, shows an anomaly in the binding of its β-phosphate, which is displaced from the P loop by ~0.4 Å. This may be the result of constraints in the conformation of the TP_4A molecule that do not occur with separate substrates. In the closed Lid ADP-Thy structure, Arg196 from the Lid region makes hydrogen bonds to the β-phosphate; this doesn't occur in the TP_4A and TP_5A structures, in which all the Lids are open. The HSV1-TK ATP/ADP binding site has been described earlier (Wild et al., 1997).

Comparing and Contrasting EHV4-TK and HSV1-TK

Although the overall sequence identity is just 36%, the crystal structures of EHV4-TK and HSV1-TK overlap very well (Figure 4A). The most visible difference is the differ-

ent position and sequence of helix α10 in the EHV4-TK and HSV1-TK structures. Also, translations of helices α3, α4, α8, and α12 are evident. The binding pockets, however, have much in common. Both enzymes depend on a glutamine residue (Gln102 in EHV4-TK, Gln125 in HSV1-TK) to position the phosphoryl-accepting substrate via two side-by-side hydrogen bonds. The O5′ of the deoxyribose, the site of phosphorylation in the Thy → TMP reaction, binds to a conserved glutamic acid residue in both structures (Glu60 in EHV4-TK and Glu83 in HSV1-TK). The P loops align very well (Figure 4B): the distances between the Cα atoms range from 0.1 to 0.7 Å.

The most obvious difference in the nucleoside binding pockets of HSV1-TK and EHV4-TK is at the thymine binding site, specifically the presence of Phe105 in EHV4-TK where the analogous residue in HSV1-TK is Met128. Pilger and coworkers (Pilger et al., 1999) created a Met128Phe mutation of HSV1-TK that not only lost the ability to phosphorylate antiherpetic prodrugs, but also lost its natural thymidine kinase function. Modeling this mutation in the binding pocket of HSV1-TK (data not shown) reveals that the likely reason that this mutation failed to improve phosphorylation was steric interference between the introduced phenyl group and Ile100. While the corresponding residue in EHV4-TK is also an isoleucine (Ile77), it does not interfere with Phe105 because the Cα traces of EHV4-TK and HSV1-TK differ by 1.3 Å here, a distance ensuring that there is enough room for the phenyl group and the isoleucine. We predicted that the double mutant of HSV1-TK with Met128Phe and Ile100Ala, to make more room for the phenyl side chain, would display enhanced phosphorylation activity toward most substrates. Preliminary kinetic results indicate that while the k_{cat} for GCV does indeed increase by a factor of 2 with respect to the wild-type, the K_M increases by a factor of 14 (HSV1-TK WT-GCV k_{cat}= 0.17 s^{-1}, K_M = 56.4 μM; HSV1-TK-I100A/M128F-GCV k_{cat}=0.36 s^{-1}, K_M = 796 μM). We are currently using our EHV4-TK structure to design additional mutations in HSV1-TK to understand what factors determine the lower K_M observed with the equine herpes enzyme.

Discussion

Structural Basis for the Dual Activity of Herpesvirus TKs

A remarkable and unique property of herpes thymidine kinases is their ability to act as both thymidine kinases (TKs) and thymidylate kinases (TMPKs). Herpesvirus TKs have an evolutionary relationship with TMPKs, as seen from sequence similarity (Figure 1B), especially the DRY/H/F motif, and structural similarities (1.6 Å RMSD over 135 atoms used for overlay); it is likely that the TMPK activity of the herpesvirus TKs reflects this relationship. Many of the secondary structural elements are present in both kinases. Despite these similarities, TMPKs possess high substrate specificity and are totally devoid of any thymidine kinase activity. The focus of the work presented here is to probe the structural features present in herpesvirus TKs that are responsible for the dual-phosphorylation activity of these kinases. We are in a unique position to do this by comparing the crystal structures of EHV4-TK in complex with TP_4A or TP_5A, and the structures of HSV1-TK in complex with TP_5A and TMP-ADP (Wild et al., 1997). Earlier analyses of the dual activity of HSV1-TK were based only on two- and three-phosphate conformations, and did not include a four-phosphate complex. As such, they are incomplete.

As described in the results section, we used TP_4A and TP_5A as bisubstrate analogs. In each complex structure, one phosphate group made no interaction with the enzyme. Further, that same phosphate group was in a position incompatible with phosphoryl-group transfer. This phosphate was dubbed the "linker" phosphate, and we concluded that our complexes mimicked the ADP-TMP and ATP-TMP states.

So how do herpesvirus TKs accommodate both ADP-TMP and ATP-TMP in the active site? The difference in linear size between a Michaelis complex of ADP-TMP and that of ATP-TMP is ~2.5 Å. Comparison of the EHV4-TK structure with TP_5A to that with TP_4A, and the HSV1-TK structure with TP_5A to that with ADP-TMP (Wild et al., 1997), reveals that the mechanisms of the accommodation differ. As predicted by Wild et al., the TMP phosphate is displaced in HSV1-TK (Wild et al., 1997). For EHV4-TK, the answer lies not in one, but rather in several substrate conformational changes that compensate for the increased size of ATP over ADP (or TDP over TMP). Figure 5 shows superimposed views of three- and four-phosphate configurations of HSV1-TK and EHV4-TK.

Notably, the position of the thymine base is unchanged between the different structures of HSV1-TK and EHV4-TK. The most noticeable change is in the position of the phosphate group closest to the thymidine. In HSV1-TK, this phosphate shifts by ~2.3 Å (slightly greater than the 1.5–2 Å shift predicted by Wild et al.) between the ADP-TMP and the ATP-TMP (i.e., TP_5A) complexes, while the adenine-to-thymine distance (measured between N9 of adenine and N1 of thymine) remains virtually unchanged (17.4 Å versus 17.7 Å). Thus, in HSV1-TK the extra bulk of the four-phosphate configuration is almost completely accommodated by this rotation of the phosphate group. While such a rotation is also observed for the EHV4-TK, it is only ~1.2 Å in magnitude (comparing the complex that mimics the ATP-TMP state (i.e., TP_5A) to the ADP-TMP state (i.e., TP_4A). The remaining bulk of the additional phosphate is accommodated by a shift of the adenosine moiety. In the ADP-TMP complex, the adenine-to-thymine distance is ~0.9 Å shorter than in the ATP-TMP complex (16.8 Å versus 17.7 Å). Since ATP is bound by the P loop, we looked for a concomitant P loop shift with the ATP's phosphates, but such a shift was not detected at the resolution of our structures. This implies that to some extent, in EHV4-TK the ATP has flexibility in its position relative to its binding loop. The consequences of this flexibility present a topic for future study.

As discussed above, the single most dramatic substrate conformational change between the state with TMP bound as a product and that with TMP bound as a reactant is the position of the TMP's phosphate group. A comparison of herpesvirus TKs to the structurally similar TMPKs can explain the flexibility of this phosphate group to occupy different positions. In TMPKs, the TMP

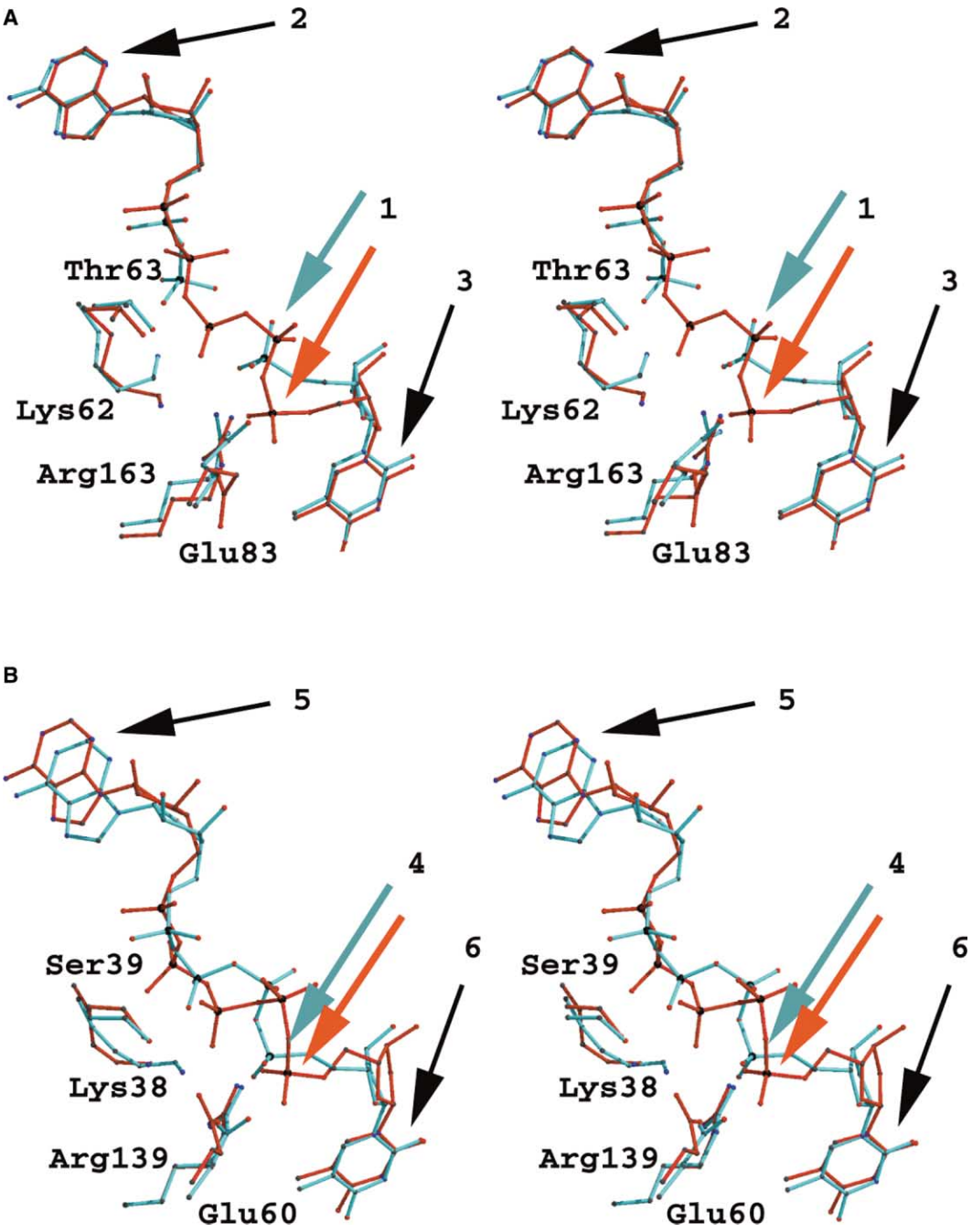

Figure 5. Structures of the Active Sites

(A) The structures of the active site of HSV1-TK complexed with TMP and ADP (Wild et al., 1997) (cyan) and with TP_5A (red), compared with (B) the active site of EHV4-TK complexed with TP_4A (cyan) and TP_5A (red) show that a phosphate group must move for a thymidylate kinase reaction to occur. In HSV1-TK, the TMP phosphate group (arrow 1) is offset 2.3 Å, while the adenine (arrow 2) and thymine (arrow 3) bases superimpose very well. In EHV4-TK, the phosphate motion is less dramatic (arrow 4), and additional conformational changes also take place, including movement of the adenine bases (arrow 5), but not of the thymine base (arrow 6).

phosphate group is sandwiched between two arginine residues, namely Arg45 and Arg97 in the human TMPK. In contrast, in herpesvirus TKs only a single arginine interacts with this phosphate group—Arg139 in EHV4-TK, Arg163 in HSV1-TK (corresponding to Arg97 in TMPK). The remaining position is occupied by a methionine residue (EHV4-TK Met62 and HSV1-TK Met85) instead of an arginine and the Cα traces differ by 3.5 Å in this region. We propose that this difference in phosphate binding permits the added flexibility needed in herpesvirus TKs to catalyze both TMP and Thy phosphorylation.

Reasons for EHV4-TK's Superior GCV Phosphorylating Activity

Given the differences between thymidine and ganciclovir and the fact that neither HSV1-TK nor EHV4-TK

can phosphorylate deoxyguanosine (dG), it is remarkable that these TKs can in fact phosphorylate the ribose-modified guanosine analogs GCV and acyclovir (ACV). Clashes are apparent when a model of a dG molecule is positioned in the binding pocket of EHV4-TK. We chose a standard *trans* configuration of the dG molecule, and aligned the deoxyribose moiety of the dG model with the deoxyribose group of a Thy molecule, so that the O5′ oxygen would be in a suitable position for reaction. In this conformation, though, the guanine base would clash with Gln125. It is the rigidity of dG's deoxyribose group that prevents it from adopting a productive binding mode in the active site.

In GCV, the flexibility of the disrupted ribose group allows the guanine base more freedom of position relative to the atoms involved in binding. In order to fit into HSV1-TK's binding pocket, the guanine base of GCV must adopt an angled conformation relative to a thymine base (Brown et al., 1995). The side-by-side hydrogen bonds at Gln125 are present in the GCV structure, but offset, with the glutamine side chain rotated to permit its OE1 side chain atom to hydrogen bond to two of the guanine's acidic N atoms (see Scheme 5 below). Other interactions (not shown in Scheme 5) contribute to binding as well. The guanine's carbonyl makes a hydrogen bond to Arg176. The O3′-equivalent atom of the modified ribose moiety is able to hydrogen bond to Tyr101, His58, and Glu225. The O5′-equivalent atom makes hydrogen bonds to Arg163 (in the DRY/F/H motif) and Arg222 (in the Lid region).

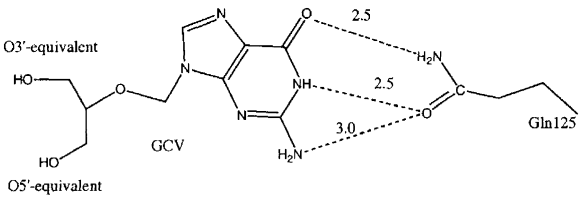

Scheme 5. GCV Binding to HSV1-TK

Although we have no structure of EHV4-TK with bound GCV, we were able to model a GCV molecule into the binding site and attempted to rationalize why its activation by EHV4-TK might be faster than that by HSV1-TK (Loubiere et al., 1999). By analogy with the binding pocket of HSV1-TK, we would expect hydrogen bonds between Glu201 and the O3′-equivalent atom as well as paired hydrogen bonds between the guanine base and Gln102. Important interactions seen in HSV1-TK that cannot happen in EHV4-TK include Tyr101 (the analogous Tyr78 points *away* from the binding pocket in closed-Lid conformations of EHV4-TK) and His58 to the O3′-equivalent atom. Further, EHV4-TK could make additional interactions via Glu60 to the O5′-equivalent atom, which does not occur in HSV1-TK despite the analogous Glu83. However, the most prominent difference lies in the "nucleoside sandwich" formed by residues Phe105 and Phe148 of EHV4-TK. Such a sandwich interaction is not possible in HSV1-TK due to the equivalent residue to EHV4-TK-Phe105 being a methionine (Met128). To test the hypothesis that this "sandwich interaction" makes EHV4-TK superior to HSV1-TK for GCV phosphorylation, we mutated HSV1-TK so as to mimic EHV4-TK, taking into consideration the concomitant requirement to modify Ile100 to a smaller residue. As expected, the Met128Phe-Ile100Ala HSV1-TK double mutant is active and is in fact faster with GCV than wild-type enzyme, albeit at a cost of a higher K_M. In HSV1-TK-bearing murine and human cells, the IC_{50} (the GCV concentration at which 50% inhibition of cell proliferation is observed in comparison to parental cells) for GCV is ~0.2 μM (Loubiere et al., 1999), and therapeutic plasma concentrations of GCV are usually less than 10 μM. As these concentrations are well below K_M for both the wild-type and the double mutant and thus in the pseudo-linear portion of the Michaelis-Menten plot, cells expressing the HSV1-TK(I100A/M128F) mutant would be expected to display a higher IC_{50} (and thus less cell killing at a given dosage) than the wild-type HSV1-TK. The mutant is therefore unlikely to be an improvement over wild-type HSV1-TK for suicide gene therapy applications. We are currently testing by mutagenesis the role of the "nucleoside sandwich" in EHV4-TK.

The phosphorylation of GCV-MP to GCV-diphosphate (GCV-DP) is catalyzed by guanylate kinase and not by the viral TKs. In contrast, TMP is efficiently converted to TDP by viral TKs. Analysis of our EHV4-TK-GCV model shows no obvious steric interactions prohibiting the phosphorylation of GCV-MP to GCV-DP. We attribute the lack of such activity to the flexibility of the disrupted-ribose group.

Conclusions

The three-dimensional structures of EHV4-TK in complex with TP_4A and TP_5A reveal the features that enable it to phosphorylate Thy → TMP and TMP → TDP. Viral TKs are more flexible in their phosphate binding modes than TMPK. A combination of a rotation of the TMP phosphate group and a shift of the adenine base makes room for the bulkier substrate in the second phosphorylation reaction in the binding pocket. In HSV1-TK a larger rotation of the TMP phosphate is observed without a concomitant adenine base shift. A key difference between EHV4-TK and HSV1-TK is the presence of a "nucleoside sandwich" only in the former. This can explain the higher GCV phosphorylation rate of EHV4-TK vis-à-vis HSV1-TK. This information has been used to generate an HSV1-TK mutant with improved turnover rate with GCV. Further modifications to this mutant that result in a lower K_M will make it an attractive option for suicide gene therapy applications.

Experimental Procedures

Protein Expression and Purification

The cloning of EHV4-TK and EHV4-TK-Δ22N is described elsewhere (C.M. et al., unpublished data). We chose to use the Δ22N truncation to improve crystal growth. In HSV1-TK structures, the first 34 residues are sensitive to thrombin cleavage and electron density for residues 35–45 were missing. We thus chose a construct of EHV4-TK that would omit analogous residues. The truncated segment is not required for catalysis, as verified by kinetic assay. The EHV4-TK-Δ22N enzyme was expressed as a fusion protein (MBP-His_6-TK). The protein was expressed in *E. coli* BL21 C41 (DE3) for ~24 hr at 18°C after induction (at an OD_{600} of 0.8) with 1 mM IPTG in 2YT medium.

For purification, the cells were centrifuged at 4000 × g for 30 min, collected as pellet, resuspended in a wash buffer (50 mM Tris-HCl [pH 7.5], 100 mM KCl), then recentrifuged. Cells were lysed by a

freeze-thaw cycle in a lysis buffer (50 mM Tris-HCl [pH 7.8], 1% Triton, 500 mM KCl, 10% glycerol, 0.5 mM PMSF, 5 mM β-mercaptoethanol, and 0.5 mg/mL lysozyme) followed by homogenization with a Teflon-piston assembly. The lysed cells were then stirred with DNase (10 U/mL). After ultracentrifugation (1 hr at 40 k rpm), the supernatant was loaded onto a TALON chelating column (CLONTECH) charged with Co^{2+} ions. The column was washed with 300 ml of Talon Wash Buffer (50 mM Tris-HCl [pH 8.0], 300 mM KCl, 10% glycerol, 0.5% Triton). Following a preelution with a lower-salinity buffer, the fusion protein was eluted with a step gradient of 0-10-100 mM imidazole in preelution buffer. The eluted protein was then treated with reducing agent (5 mM DTT) and loaded onto a WP-QUAT anion-exchange column, washed overnight with 300 ml buffer (25 mM Tris-HCl [pH 8.0], 25 mM KCl, 10% glycerol, 0.5% Triton, 5 mM DTT), and then eluted via a 200 ml gradient to a final [KCl] of 175 mM. The protein eluted at 150 mM [KCl]. The fusion protein was concentrated to ~5 mg/mL. Thrombin (20 U/mL) and nucleotides (250 μM thymidine and 500 μM ADP, plus 5 mM $MgCl_2$) were added. The cutting mixture was rocked at 4°C for 4 days, then dialyzed against a nonreducing buffer. The mixture of cut and uncut protein was then loaded onto a TALON column and the cut EHV4-TK-Δ22N was collected as flow through. After concentration to 10 mg/mL, the enzyme was further purified via gel filtration.

Kinetics

Data were collected by the spectrometric assay (Agarwal et al., 1978) of a coupled pyruvate-NADH system with a Varian Cary 50 Bio spectrophotometer. Additional information was collected by HPLC assay (C.M. et al., unpublished data).

Crystallization

Crystals of all complexes were grown by hanging-drop vapor diffusion. The reservoir solution for the ADP-Thy complex consisted of 0.1 M 2-(N-morpholino)ethanesulfonic acid (MES), pH 6.5, 1.2 M ammonium sulfate, and 5% dioxane. The enzyme solution consisted of EHV4-Δ22N-TK at a concentration of 5.5 mg/mL, 1.0 mM TMP, 2.0 mM ADP, 25 mM HEPES (pH 7.0), 5 mM $MgSO_4$, 5 mM DTT, 100 mM KCl, and 5% glycerol. One microliter of reservoir solution was added to 1 μl of enzyme solution on a glass cover slide. Crystals grew as rectangular plates. A thicker plate 0.2 mm in length was selected for data collection. This crystal was immersed in a cryosolvent consisting of 2.0 M ammonium sulfate, 0.1 M MES, 5% dioxane, and 20% ethylene glycol ("CRYO1") for approximately 20 s.

The reservoirs for the TP_4A and TP_5A (Jena Bioscience GmbH) complexes consisted of 1.2 M ammonium sulfate, 0.1 M MES, and 3% dioxane. The crystals grew as rectangular solids *via* streak-seeding from plates. Crystals approximately 0.3 mm in length were selected for data collection, then immersed in CRYO1 prior to flash freezing.

Data Collection, Solution, and Refinement

Data for all crystals were collected on the BIOCARS 14-BM-C at a wavelength of 0.9 Å and a temperature of 100 K. The frames were indexed with the program DENZO, and then merged and scaled with SCALEPACK (Otwinowski and Minor, 1997). Collection and refinement conditions are given in Table 1.

The structure of the ADP-Thy complex was solved by molecular replacement using MOLREP (Vagin and Teplyakov, 1997). The search model was constructed from HSV1-TK (Vogt et al., 2000) by performing sequence alignment with EHV4-TK, deleting the N-terminal region, deleting insertions, and modifying non-equivalent residues to alanines. CNS (Brünger et al., 1998) was used for rigid body refinement of secondary structural elements, followed by minimization and simulated annealing with NCS averaging. R_{free} after the first refinement cycle was 43%. After three cycles of rebuilding with O (Jones et al., 1991) and refinement with CNS, NCS constraints were removed. After four cycles, R_{free} had decreased to 25.5%. The final three refinement cycles were performed with REFMAC (Collaborative Computational Project, 1994).

The remaining structures were solved by molecular replacement with AmoRe or MOLREP (Vagin and Teplyakov, 1997) using the ADP-Thy structure as a search model.

Acknowledgments

A.S.G. and A.L. are supported by a grant from the National Science Foundation. C.M. and M.K. are supported by the Deutsche Forschungsgemeinschaft and the Max-Planck-Gesellschaft. Use of the Advanced Photon Source was supported by the U.S. Department of Energy, Basic Energy Sciences, Office of Science, under Contract No. W-31-109-Eng-38. Use of the BioCARS Sector 14 was supported by the National Institutes of Health, National Center for Research Resources, under grant number RR07707.

Received: February 27, 2003
Revised: May 1, 2003
Accepted: May 27, 2003
Published: September 30, 2003

References

Agarwal, K.C., Miech, R.P., and Parks, R.E., Jr. (1978). Guanylate kinases from human erythrocytes, hog brain, and rat liver. Methods Enzymol. *51*, 483–490.

Bennett, M.S., Wien, F., Champness, J.N., Batuwangala, T., Rutherford, T., Summers, W.C., Sun, H., Wright, G., and Sanderson, M.R. (1999). Structure to 1.9 Å resolution of a complex with herpes simplex virus type-1 thymidine kinase of a novel, non-substrate inhibitor: X-ray crystallographic comparison with binding of aciclovir. FEBS Lett. *443*, 121–125.

Brown, D.G., Visse, R., Sandhu, G., Davies, A., Rizkallah, P.J., Melitz, C., Summers, W.C., and Sanderson, M.R. (1995). Crystal structure of the thymidine kinase from herpes simplex virus type-I in complex with dexoythymidine and Ganciclovir. Nat. Struct. Biol. *2*, 876–881.

Brown, N.P., Leroy, C., and Sander, C. (1998). MView: a web-compatible database search or multiple alignment viewer. Bioinformatics *14*, 380–381.

Brünger, A.T., Adams, P.D., Clore, G.M., Delano, W.L., Gros, P., Grosse-Kunstleve, R.W., Jiang, J.-S., Kuszewskli, J., Nilges, N., Read, R.J., et al. (1998). Crystallography and NMR system (CNS): a new software system for macromolecular structure determination. Acta Crystallogr. *D54*, 905–921.

Champness, J.N., Bennett, M.S., Wien, F., Visse, R., Summers, W.C., Herdewijn, P., de Clerq, E., Ostrowski, T., Jarvest, R.L., and Sanderson, M.R. (1998). Exploring the active site of herpes simplex virus type-1 thymidine kinase by X-ray crystallography of complexes with aciclovir and other ligands. Proteins *32*, 350–361.

Chen, M.S., and Prusoff, W.H. (1978). Association of thymidylate kinase activity with pyrimidine deoxyribonucleoside kinase induced by herpes simplex virus. J. Biol. Chem. *253*, 1325–1327.

Chen, M.S., Summers, W.P., Walker, J., Summers, W.C., and Prusoff, W.H. (1979). Characterization of pyrimidine deoxyribonucleoside kinase (thymidine kinase) and thymidylate kinase as a multifunctional enzyme in cells transformed by herpes simplex virus type 1 and in cells infected with mutant strains of herpes simplex virus. J. Virol. *30*, 942–945.

Collaborative Computational Project (1994). The CCP4 Suite: Programs for Protein Crystallography. Acta Crystallogr. *D50*, 760–763.

Elion, G.B., Furman, P.A., Fyfe, J.A., de Miranda, P., Beauchamp, L., and Schaeffer, H.J. (1977). Selectivity of action of an antiherpetic agent, 9-(2-hydroxyethoxymethyl) guanine. Proc. Natl. Acad. Sci. USA *74*, 5716–5720.

Esnouf, R. (1997). An extensively modified version of molscript that includes greatly enhanced coloring capabilities. J. Mol. Graph. *15*, 133–138.

Johansson, K., Ramaswamy, S., Ljungcrantz, C., Knecht, W., Piskur, J., Munch-Petersen, B., Eriksson, S., and Eklund, H. (2001). Structural basis for substrate specificities of cellular deoxyribonucleoside kinases. Nat. Struct. Biol. *8*, 616–620.

Jones, T.A., Zhou, J.-Y., Cowan, S.W., and Kjeldgaard, M. (1991). Improved methods for building protein models in electron density maps and the location of errors in these models. Acta Crystallogr. A *47*, 110–119.

Kraulis, P.J. (1991). MOLSCRIPT: a program to produce both detailed and schematic plots of protein structures. J. Appl. Crystallogr. *24*, 946–950.

Loubiere, L., Tiraby, M., Cazaux, C., Brisson, E., Grisoni, M., Zhao-Emonet, J., Tiraby, G., and Klatzmann, D. (1999). The equine herpes virus 4 thymidine kinase is a better suicide gene than the human herpes virus 1 thymidine kinase. Gene Ther. *6*, 1638–1642.

Matthews, T., and Boehme, R. (1988). Antiviral activity and mechanism of action of ganciclovir. Rev. Infect. Dis. Suppl. *10*, S490–S494.

Merrit, E.A., and Murphy, M.E.P. (1994). Raster3D version 2.0—a program for photorealistic molecular graphics. Acta Crystallogr. *D50*, 869–873.

Ostermann, N., Schlichting, I., Brundiers, R., Konrad, M., Reinstein, J., Veit, T., Goody, R.S., and Lavie, A. (2000). Insights into the phosphoryltransfer mechanism of human thymidylate kinase gained from crystal structures of enzyme complexes along the reaction coordinate. Structure *8*, 629–642.

Otwinowski, Z., and Minor, W. (1997). Processing of X-ray data collected in oscillation mode. In Methods Enzymology, Vol. 276, C.W. Carter Jr., R.M. Sweet, J.N. Abelson, eds. (San Diego, CA: Academic Press), pp. 307–326.

Pilger, B.D., Perozzo, R., Alber, F., Wurth, C., Folkers, G., and Scapozza, L. (1999). Substrate diversity of herpes simplex virus thymidine kinase. Impact Of the kinematics of the enzyme. J. Biol. Chem. *274*, 31967–31973.

Prota, A., Vogt, J., Pilger, B., Perozzo, R., Wurth, C., Marquez, V.E., Russ, P., Schulz, G.E., Folkers, G., and Scapozza, L. (2000). Kinetics and crystal structure of the wild-type and the engineered Y101F mutant of Herpes simplex virus type 1 thymidine kinase interacting with (North)-methanocarba-thymidine. Biochemistry *39*, 9597–9603.

Reardon, J.E. (1989). Herpes simplex virus type 1 and human DNA polymerase interactions with 2′-deoxyguanosine 5′-triphosphate analogues. Kinetics of incorporation into DNA and induction of inhibition. J. Biol. Chem. *264*, 19039–19044.

Sekulic, N., Shuvalova, L., Spangenberg, O., Konrad, M., and Lavie, A. (2002). Structural characterization of the closed conformation of mouse guanylate kinase. J. Biol. Chem. *277*, 30236–30243.

St. Clair, M.H., Lambe, C.U., and Furman, P.A. (1987). Inhibition by ganciclovir of cell growth and DNA synthesis of cells biochemically transformed with herpesvirus genetic information. Antimicrob. Agents Chemother. *31*, 844–849.

Thompson, J.D., Higgins, D.G., and Gibson, T.J. (1994). CLUSTAL W: improving the sensitivity of progressive multiple sequence alignment through sequence weighting, position-specific gap penalties and weight matrix choice. Nucleic Acids Res. *22*, 4673–4680.

Vagin, A., and Teplyakov, A. (1997). MOLREP: an automated program for molecular replacement. J. Appl. Crystallogr. *30*, 1022–1025.

Vogt, J., Perozzo, R., Pautsch, A., Prota, A., Schelling, P., Pilger, B., Folkers, G., Scapozza, L., and Schulz, G.E. (2000). Nucleoside binding site of herpes simplex type 1 thymidine kinase analyzed by X-ray crystallography. Proteins *41*, 545–553.

Vonrhein, C., Schlauderer, G.J., and Schulz, G.E. (1995). Movie of the structural changes during a catalytic cycle of nucleoside monophosphate kinases. Structure *3*, 483–490.

Wild, K., Bohner, T., Folkers, G., and Schulz, G.E. (1997). The structures of thymidine kinase from herpes simplex virus type 1 in complex with substrates and a substrate analogue. Protein Sci. *6*, 2097–2106.